PPPL-3148 - Preprint Date: January 1996, UC-420, 427

First Observation of Alpha Particle Loss Induced by Kinetic Ballooning Modes in TFTR DT Experiments

Zuoyang Chang[1], R. V. Budny[1], L. Chen[2], D. Darrow[1], E. D. Fredrickson[1], A. Janos[1], D. Mansfield[1], E. Mazzucato[1], K. M. McGuire[1], R. Nazikian[1], G. Rewoldt[1], J. D. Strachan[1], W. M. Tang[1], G. Taylor[1], R. B. White[1], S. Zweben[1] and the TFTR group

[1]Plasma Physics Laboratory, Princeton University, Princeton, NJ 08543
[2]Department of Physics, University of California, Irvine, CA, 92717-4575

(October 3, 1995)

abstract

A correlation between the measured alpha particle loss and high frequency (~100-200 kHz) modes has been observed in some high β (=plasma pressure/magnetic pressure) DT plasmas in TFTR. These modes are localized around the peak plasma pressure gradient and have ballooning characteristics. An enhancement of 30% in the alpha particle loss correlated with a bursting mode and a factor of 2 enhancement correlated with multiple modes are observed. Linear instability analysis and particle simulation show that the plasma is unstable to the kinetic MHD ballooning modes and the loss is due to wave-particle resonances.

PACS numbers: 52.55.Pi, 52.35.Py, 52.65.+z

(Revised version to be published in Phys. Rev. Lett. Jan 22, 1996.)

Study of MHD effects on alpha particle confinement is one of the most important subjects in the recent deuterium-tritium (DT) fusion research in the Tokamak Fusion Test Reactor (TFTR). It has been theoretically predicted[1] that energetic alpha particles (E_α o(<,~) 3.5 MeV) can either drive or resonate with plasma MHD fluctuations. This kind of wave-particle interaction can induce direct alpha loss and therefore has a potentially important impact on present and future fusion tokamak devices.

In a recent high β, high power DT experiment[2], good correlation was found between high frequency MHD modes and the measured alpha losses. A general study of the high frequency MHD modes in normal TFTR supershot plasmas can be found in Ref.[3]. This paper will focus on the first observation of the alpha particle losses correlated with these modes.

Figure 1 shows one of the highest performance discharges achieved using intensive Lithium wall-conditioning[2]. Some measured parameters are (in conventional notation): I_p=2.1 MA, B_t= 5.1 T, P_B=21 MW, R=2.52 m, a=0.87 m, q_a ~ 4.6, τ_E ~ 0.28 sec, $T_i(0)$ ~ 38 keV, $T_e(0)$ ~ 12 keV, $n_e(0)$ ~8.2x10^{19} m^{-3} , P_{fusion} ~5.5 MW, β_N ~ 1.7. Large bursts of alpha loss as well as large fluctuations in the lost-alpha signal are observed around the peak performance phase as shown in Fig. 1(c). The alpha loss is measured by a detector located at the bottom of the limiter chamber (90^o detector)[4]. It is found that these bursts (at t=4.3 , 4.4 and 4.46 sec) correspond to bursts of the high frequency MHD modes and lead to a performance degradation (for details, see Ref.[2]). This discharge suffered a high-β minor disruption at 4.55 sec, which terminated the enhanced confinement phase. This indicates that the plasma was near the beta limit. The high frequency MHD modes are observed at the peak performance phase (t=4.20 - 4.55 sec). They are detected by the multichannel ECE polychromator arrays[5] and by the external magnetic probes[6].
According to their different characteristics, the high frequency modes can be further divided into two different modes in this discharge. One is the multi-frequency quasi-continuous mode observed during the burst of alpha loss, e.g. , the t_1 window in Fig. 1. The other one is the bursting (or intermittent) mode observed between the alpha bursts, e.g. ,the t_2 window in Fig. 1.

(1) *Multi-frequency quasi-continuous modes*

Figure 2(a) shows the contour plot of the frequency spectrum of δT_e measured from an ECE channel (R~ 300 cm or r/a~ 0.34). Multi-frequency quasi-continuous modes with frequency up to 250 kHz are observed. They correlate with an enhance-

ment of a factor of 2 above the background level in the lost- α signal. Here, the background loss is mainly from the first orbit loss[4], which is about 3% of the total alpha production rate. The measured escaping alpha particles have energy close to 3.5 MeV. Time evolution traces of the α -loss signal and different modes (n=3, 6, 7, 8, 9) are shown in Fig. 2(b). Here, the toroidal mode numbers n=3, 6, 7 are measured from the magnetic coils. The rest are extrapolated based on the frequency spacing of the modes. Calculation of linear cross correlation coefficient C shows that the fluctuations in the α -loss signal correlate better with the n=6 and 8 modes. Here, the correlation coefficient C between series x_i and y_i is defined as

$$C \equiv \phi(\Sigma_i(x_i - o(\bar{},x))(y_i - o(\bar{},y)), r(\Sigma_i(x_i - o(\bar{},x))^2) r(\Sigma_i(y_i - o(\bar{},y))^2)) \quad , \qquad (1)$$

where $o(\bar{},x)$ and $o(\bar{},y)$ are the means. For the specified time window, we found that C~ 0.27 for n=6 , 0.34 for n=8 , 0.15 for n=7 , 0.05 for n=9, and 0.02 for n=3. This result seems to indicate that the n=6 and 8 modes play a dominant role in the wave-particle interaction process despite the fact that other modes have comparable fluctuation amplitudes. Among the four alpha loss detectors located at different poloidal angles, 20^o, 45^o , 60^o, and 90^o below the outer midplane, the loss bursts can be seen in the bottom three detectors but only the 90^o detector shows the correlation described above. This correlation becomes much clearer in the following bursting mode case.

(2) *Bursting mode*

Between the large loss bursts, the 90^o detector also shows some lower level intermittent loss enhancement. It is found that these oscillations correlate very well with a bursting mode. Figure 3(a) shows the same δT_e frequency spectrum contour plot. Only two modes are observed with n=3 and 6 (plus a very weak mode at ~200 kHz). These n numbers measured by the magnetic coils are verified by the phase correlation analysis between the two ECE grating arrays located 120^o apart toroidally. In addition, the phase symmetry of the modes measured on the inner and the outer mode locations indicates that both the n=6 and n=3 modes have even poloidal mode numbers (m).

The n=6 mode is bursting in time. A drop of ~ 14% in mode frequency is also seen on each burst. It is somewhat analogous to the beam-ion-driven fishbone mode (m=1 , n=1) routinely observed in TFTR NB-heated supershots[8], except for having much higher mode numbers and frequency. Figure 3(b) shows the time evolution of

the lost- α signal and the MHD modes. A very good correlation (with C~ 0.63) is observed between this bursting n=6 mode and the alpha loss. Each burst corresponds to a ~ 30% enhancement in the α -loss signal at the 90^o detector, or about 1% of the alpha birth rate. In contrast, the lower frequency n=3 mode shows a negative correlation with the alpha loss (C~ -0.39). Since both of the modes appear at the same spatial location, this selective correlation is evidence of frequency-dependent wave-particle resonance.

The radial mode structure measured by the ECE system is shown in Fig. 4(a) for the n=6 and n=3 modes. A ballooning character is clearly seen in the n=6 mode, i.e. , the mode amplitude is stronger in the low B field side ($R>R_0$) than the high B field side. The maximum $\delta T_e/T_e$ at R~ 300 cm (r/a~0.34) is ~ 2% . The bursting n=6 mode is observed in three ECE channels. The channel-to-channel separation is about 5-6 cm, so the mode width is about δ r o(<,~) 12 cm or $\delta r/a\sim 0.14$. It covers q~ 1.1-1.5.
In the multi-frequency case the high- n modes have a narrower width, i.e., $\delta r\sim 8$ cm or $\delta r/a\sim 0.09$. Using a transport analysis code (TRANSP[7]) we found that these modes are located at the peak value of α_{tot}, see Fig. 4(b). Here, α_{tot} is a measure of the plasma pressure gradient defined as

$$\alpha_{tot}=-R_0q^2d\beta_{tot}/dr , \qquad (2)$$

where β_{tot} is the total plasma toroidal beta (thermal plasma plus beam ions), R_0 is the magnetic axis location. The corresponding parameter for the alpha species is $\alpha_\alpha= -R_0q^2d\beta_\alpha/dr$ which is also shown in Fig. 4(b). The safety factor profile is from a TRANSP calculation. The q value at the mode location is ~ 1.3 . Therefore, the best helical mode numbers that match the even parity from the ECE measurement discussed above are respectively m/n=8/6 and m/n=4/3 . This TRANSP q profile is also partly justified by the agreement between the q=1 surface and the measured inversion radius of the minor disruption at 4.55 sec. The mode amplitude in terms of $\delta B_r/B_0$ can be estimated using the relationship $\delta B_r/B_0 \sim (1/qR)|\delta T_e/\nabla T_e|$ (since $B\cdot\nabla \sim B/ qR$ for the ballooning mode). Using Fig. 4(a) we find that the n=6 mode has $\delta B_r/B_0 \sim O(10^{-4})$.

The mode frequency in the plasma frame can be calculated by subtracting out the toroidal rotation frequency, i.e. ,

$$\omega_{MHD}=\omega_{Lab}-\omega_{V\phi} , \qquad (3)$$

where $\omega_{V\phi} = (n/R)V_\phi$, n is the toroidal mode number, and R is the mode location. Using the $V_\phi(R)$ profile measured from the Charge-Exchange Spectroscopy we find that $\omega_{V\phi}(n=6) \sim 2\pi$ (47± 5kHz) . Therefore, the mode frequency in the plasma frame is $\omega_{MHD} \sim 2\pi$ (88± 5kHz).

(3) *Particle loss simulation*

An alpha particle orbit lost to a detector can be traced back into the plasma by using the measured particle energy, pitch angle and equilibrium parameters such as the q profile. Figure 5(a) shows such an orbit. We see that particles that escape to the 90^o detector arrive on barely trapped banana orbits. The location of the high frequency mode is around the inner excursion of the banana orbit, which supports the physical assumption that the alpha particles are expelled by the MHD modes.

A guiding center code[9] was used to simulate the mode-induced particle loss. We use the experimentally observed parameters: m = 8 , n = 6 , f= 80 kHz and use $\delta B_r/B_0 = 2\text{x } 10^{-4}$. The particle distribution is a Monte-Carlo generated alpha particle slowing-down distribution, isotropic in pitch angle, with a Gaussian radial profile taken to approximate the experimental conditions. An example of induced loss of the type seen by the detector is shown in Fig. 5(b). The lost particles are counter moving (opposite to the plasma current direction) passing particles initially located at a smaller minor radius. The wave-particle resonance condition in the plasma frame can be written as $n\phi - m_d\theta - \omega_{MHD}\, t = \text{const.}$, where $m_d = m, m\pm1$. For a counter moving passing particle, $\phi = -\omega_t\, t$, $\theta = -\omega_t\, t/q$, where $\omega_t \sim |v_{||}|/R$ is the toroidal transit frequency. The resonant condition becomes

$$\omega_{MHD} \sim (m_d/q - n)\omega_t. \qquad (4)$$

The case shown in Fig. 5(b) has a resonance with $m_d=7$. The simulation shows that the particle spends only a small fraction of each poloidal transit in resonance when the orbit passes through the outer midplane. During each resonant period it can gain or lose energy to the wave in a random walk process in $v_{||}$ until it eventually diffuses into a trapped orbit. The total simulated alpha loss for a one millisecond burst of the mode is about one percent of the alpha particle population (with E~ 1.5-3.5 MeV). On the other hand, a similar simulation shows that the n=3 mode has less than half this effect due to lack of efficient wave-particle resonance. All these results are basically consistent with the observations. We have also simulated the effect of the mode

on the beam population, but observe no losses. (No beam-ion loss measurement is available in routine TFTR experiments.)

(4) *Linear stability analysis*

An MHD stability calculation for this discharge has also been carried out. First of all, we conclude that the observed high frequency modes are not the TAE (Toroidicity-induced Alfven eigenmodes)[10] because the TAE frequency is more than a factor of two higher.

Due to the strong local peaking of the pressure profile, it is found that the pressure gradient has locally exceeded the high- n ideal ballooning limit. Figure 6 shows the plasma evolution in the so-called " s - α " diagram. Here, s=rq'/q is the magnetic shear. This result suggests that the mode we observed should be related to the ballooning modes, especially to the kinetic MHD ballooning mode (KBM). [Note that these modes are different from the ideal ballooning modes observed in TFTR before high- β disruptions[11], which are toroidally localized and have larger radial extent.] The basic characteristic of the KBM[12] is that the mode frequency is close to the ion-diamagnetic frequency, i.e. ,

$$\omega_{*pi}/2<\omega_r<\omega_{*pi} \ , \qquad (5)$$

where $\omega_{*pi}=(nq/r)(v_i^2/\omega_i)(d\ln p_i/dr)$. The high frequency modes we observed are within this range[3]. For example, the n=6 ion-diamagnetic frequency (using only the thermal ions) is ~ 110 kHz , which is about $1.2\omega_{MHD}$.

A comprehensive kinetic calculation described in detail in Ref.[13] is employed to study the linear stability properties of the high- n MHD ballooning mode. This calculation used the so-called ballooning representation for high- n modes, and is fully electromagnetic. Transit frequency resonances for untrapped particles of each species, bounce frequency and magnetic drift precession frequency resonances for trapped particles of each species, full finite Larmor radius effects, and finite banana orbital dynamics are included in the calculation. For the results presented here, the finite- β MHD equilibrium is calculated numerically using experimental pressure and q -profile data. Multiple ion species are included in the calculation. Maxwellian equilibrium distribution functions are used for every species except the hot alpha particles, for which a slowing-down distribution is used.

The results for the linear growth rate γ versus r/a is shown in Fig. 7(a). Here, $k_\theta \rho_i \sim 0.2$, the value which maximizes γ at r/a=0.34 as shown in Fig. 7(b). The plasma is locally unstable to the KBM driven by
the background pressure gradient. The effect of the hot beam species is slightly stabilizing for this case, while that of the hot alpha particles is slightly destabilizing. The spatial location of the KBM is in good agreement with the experiment. The linear growth rate has a maximum at n=12 while the observed largest mode has n=6 . However, we believe that nonlinear effects can shift the peak to lower values of n [14].

In conclusion, a significant enhancement (from ~ 30% to a factor of 2) in alpha particle loss correlated with high frequency MHD modes has been observed in recent TFTR high β DT plasmas. Both the experimental measurements and particle simulation show that the observed alpha loss is induced by the wave-particle resonance between the alpha particles and the MHD modes (mainly the n=6 mode). Linear stability analysis shows that the plasma is locally unstable to the KBM driven by the strong plasma pressure gradient. Although these modes seem unlikely to be driven by α particles (similar MHD activity is observed in D-only plasmas[3]), our observation indicates that the high frequency KBM modes can have strong effects on the fusion ion confinement in the high- β regime. Therefore, attention needs to be paid to the impact of this mode on future tokamak reactors.

The authors would like to acknowledge useful discussions with J. D. Callen, C. Z. Cheng, R.J. Hawlyruk, J. Manickam, S. Sesnic, S.-T. Tsai and L. Zakharov. This research is sponsored by the U. S. Department of Energy under Contract No. DE-AC02-76-CHO-3073.

References

[1] H. P. Furth, et al., Nucl. Fusion **30**, 1799 (1990).

[2] D. Mansfield, et al., Phys. Plasmas (to be published).

[3] R. Nazikian, et al., Princeton Plasma Physics Laboratory Report No. PPPL-3140, 1995 (submitted to Phys. Plasmas).

[4] S. J. Zweben, et al., Nucl. Fusion **31**, 2219 (1991).

[5] A. Janos, et al., Rev. Sci. Instrum. **66**, 668 (1995).

[6] E. Fredrickson, et al., {Rev. Sci. Instrum.} **57**, 2084 (1986).

[7] R. V. Budny, Nucl. Fusion **34**, 1247 (1994) and references therein.

[8] R. Kaita, et al., Phys. Fluids B **2**, 1584 (1990).

[9] R. B. White and M. S. Chance, Phys. Fluids **27**, 2455 (1984); R. B. White, Phys. Fluids B **2**, 845 (1990).

[10] C. Z. Cheng, et al., Ann. Phys. (NY) **161**, 21 (1985).

[11] E. Fredrickson, et al., Phys. Plasmas (to be published).

[12] An incomplete list of references on the KBM theory: W. M. Tang, et al., Nucl. Fusion **20**, 1439 (1980); C. Z. Cheng, Phys. Fluids **25**, 1020 (1982); J. Wieland and L. Chen, Phys. Fluids **28**, 1359 (1985); H. Biglari and L. Chen, Phys. Rev. Lett. **67**, 3681 (1991); S.-T. Tsai and L. Chen, Phys. Fluids B **5**, 3284 (1993).

[13] G. Rewoldt, et al., Phys. Fluids **25**, 480 (1982); G. Rewoldt, et al., Phys. Fluids **30**, 807 (1987).

[14] S. E. Parker, et al., Phys. Rev. Lett. **71**, 2042 (1993).

Figure Caption

Fig.1. A high- β DT discharge. (a) DT fusion power. (b) Central total plasma beta $\beta_t(0)$ and the central alpha β . (c) Measured alpha particle loss rate from a 90^o detector. The high frequency modes developed in the time window indicated. Different characteristics observed at different time (e.g. , t_1 and t_2).

Fig.2. Multi-frequency quasi-continuous modes observed at the time t_1 in Fig. 1. (a) Frequency spectrum contour plot of δT_e (R~300 cm). (b) Comparison between the lost alpha signal and different modes.

Fig.3. The high frequency modes at the time t_2 in Fig. 1. (a) Same contour plot as Fig. 2(a). A bursting n=6 mode is observed. (b) A very good correlation is observed between the enhanced alpha loss and the n=6 mode. The n=3 mode shows a negative correlation.

Fig.4. (a) Radial profiles of $\delta T_e/T_e$ for the n=6 and n=3 modes.
(b) Profiles of the α parameter defined in Eq. (2) and the safety factor q . The MHD is located at the peak pressure gradient where q~ 1.3 .

Fig.5. (a) Orbit tracing of the lost alpha particles. The measured pitch angle and the particle energy (~ 3.5 MeV) are used. (b) A cross-section projection of the alpha particle orbit from a orbit simulation code. The measured mode number (m=8 , n=6), frequency (80 kHz in plasma frame), and radial profile are used. The initial energy is 3.08 MeV, pitch angle $v_{||}/v$= -0.55 .

Fig.6. The plasma evolution at r/a=0.34 cast on the s - α diagram. The high frequency MHD modes are observed from 4.20 to 4.55 sec when the plasma is approaching or exceeds the high- n ideal ballooning limit.}

Fig.7. (a) Linear growth rate γ versus r/a for the kinetically-calculated high- n MHD ballooning mode at t=4.40 sec. Here, $k_\theta \rho_i$ ~ 0.2 , and the calculation includes electrons, background ions (m_i=2.5 amu), carbon impurity ions, Maxwellian hot beam ions (m_b=2.5 amu), and slowing-down hot alpha particles. (b) γ versus $k_\theta \rho_i$ (or n) at r/a = 0.34 .

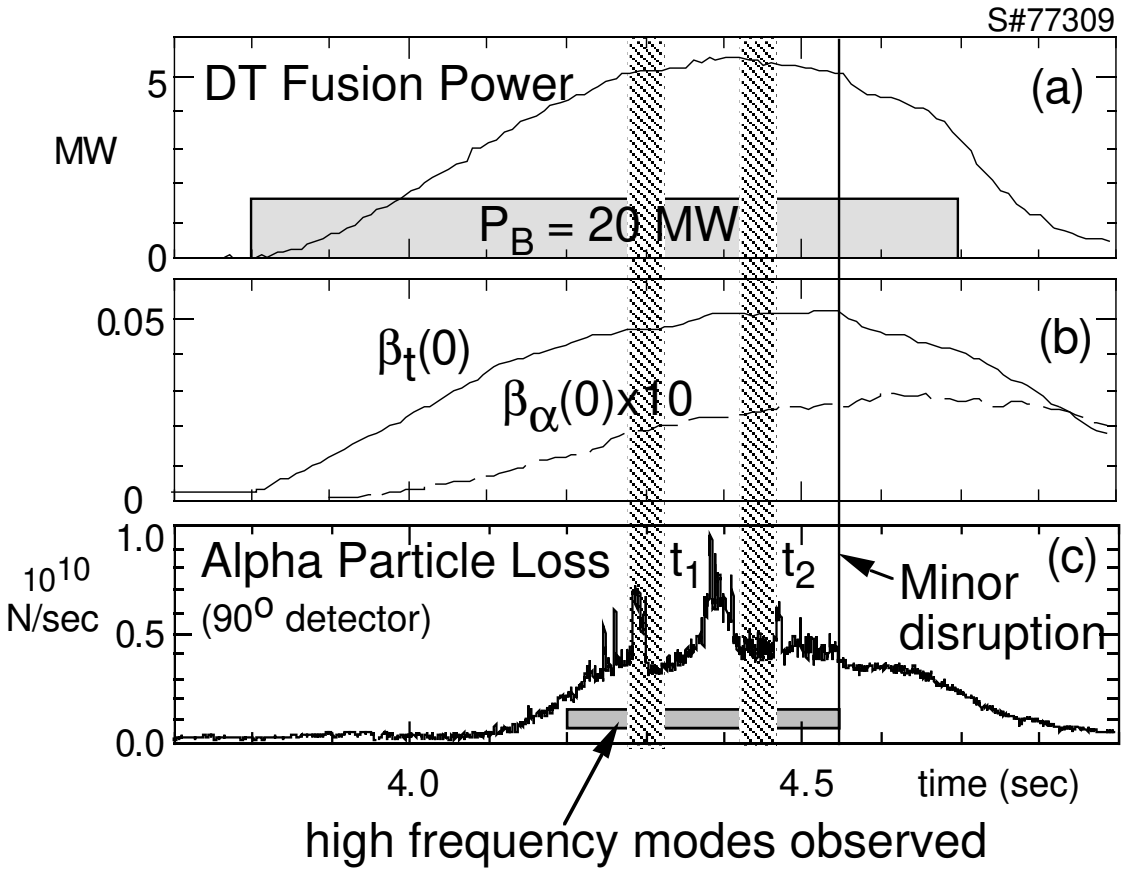
S#77309
DT Fusion Power
(a)
MW
5
0
P_B = 20 MW
0.05
$\beta_t(0)$
$\beta_\alpha(0)$x10
(b)
0
1.0
Alpha Particle Loss
t_1
t_2
(c)
10^{10}
N/sec
(90^o detector)
0.5
Minor
disruption
0.0
4.0
4.5
time (sec)
high frequency modes observed

Fig. 1

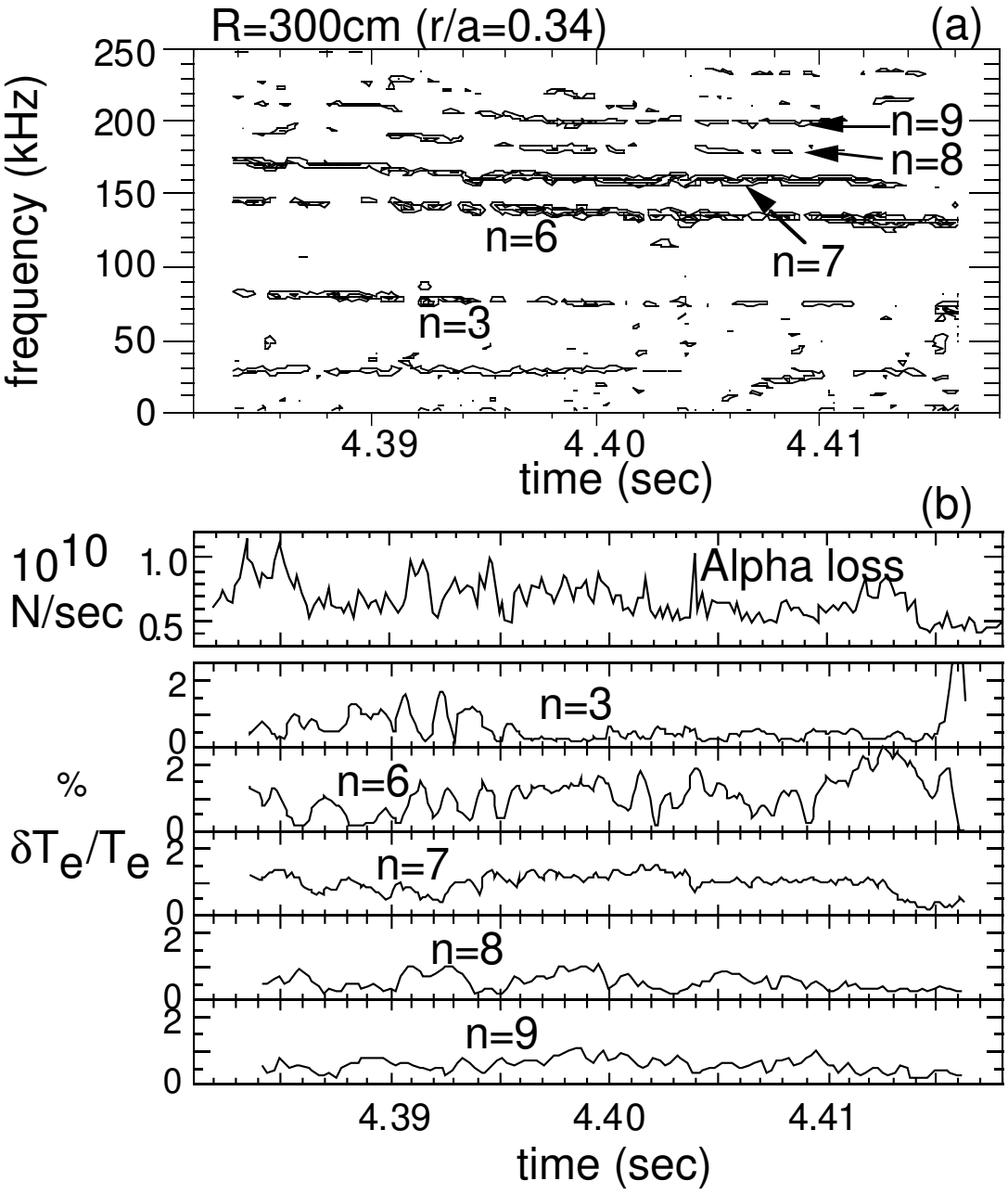
R=300cm (r/a=0.34)
(a)
frequency (kHz)
250
200
150
100
50
0
n=9
n=8
n=6
n=7
n=3
4.39
4.40
4.41
time (sec)
(b)
10^{10} N/sec
1.0
0.5
Alpha loss
%
$\delta T_e/T_e$
2
0
n=3
n=6
n=7
n=8
n=9
4.39
4.40
4.41
time (sec)

Fig. 2

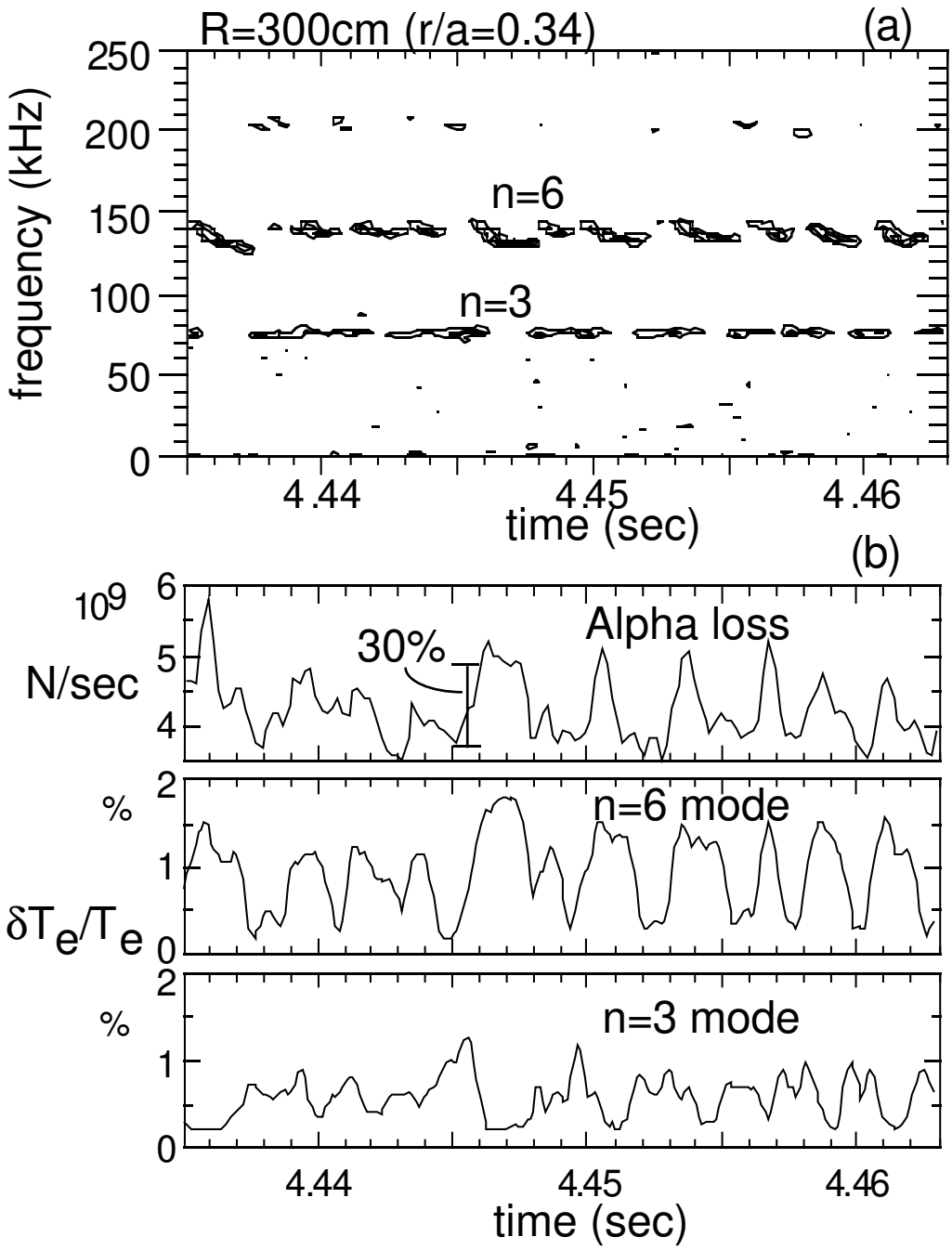
R=300cm (r/a=0.34)
(a)
frequency (kHz)
250
200
150
100
50
0
n=6
n=3
4.44
4.45
4.46
time (sec)
(b)
10^9
N/sec
6
5
4
Alpha loss
30%
%
2
1
0
n=6 mode
δT_e/T_e
%
2
1
0
n=3 mode
4.44
4.45
4.46
time (sec)

Fig. 3

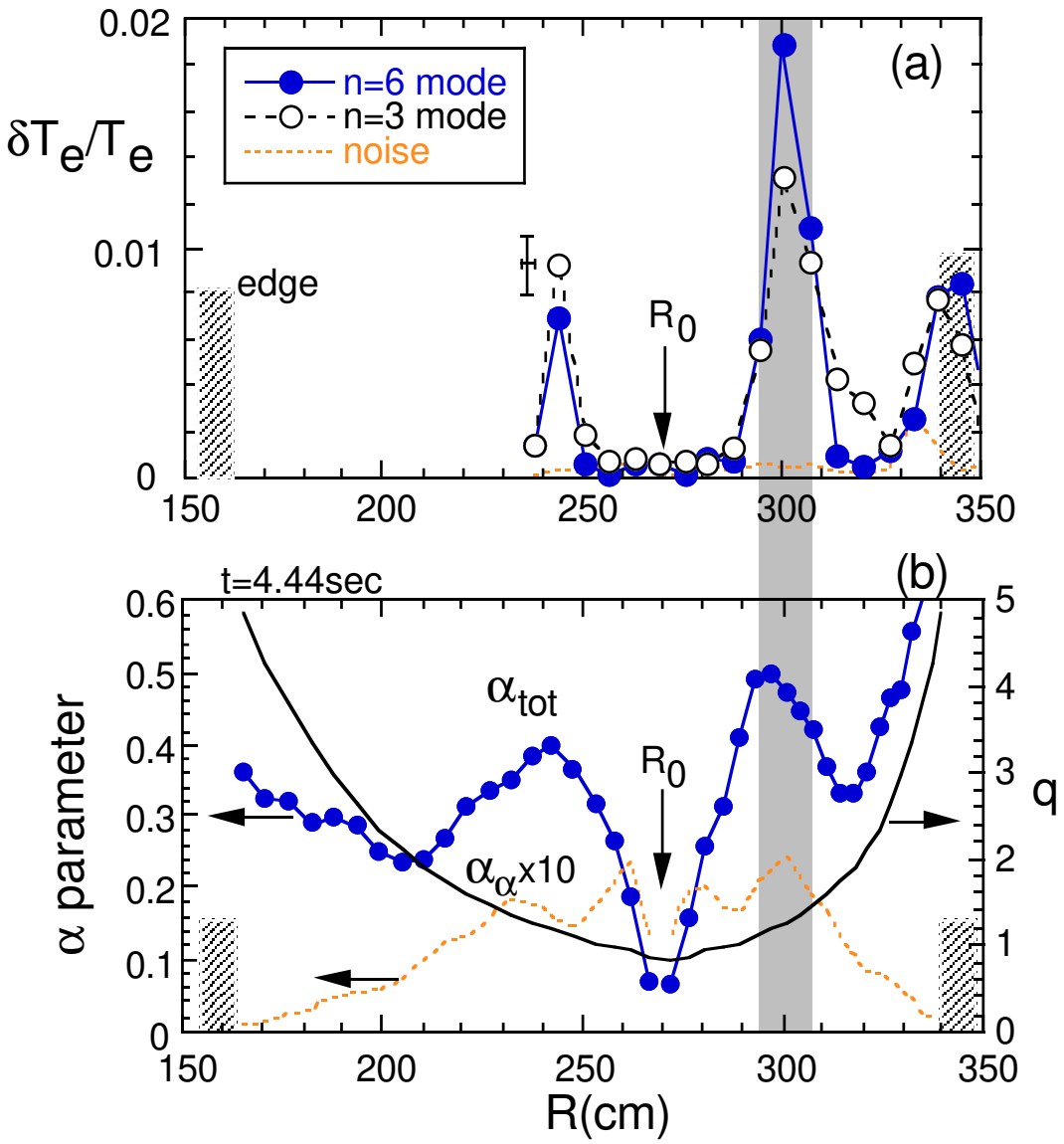
0.02
0.01
0
δT_e/T_e
n=6 mode
n=3 mode
noise
(a)
edge
R_0
150
200
250
300
350
t=4.44sec
(b)
0.6
0.5
0.4
0.3
0.2
0.1
0
α parameter
α_tot
R_0
α_α x10
5
4
3
2
1
0
q
R(cm)

Fig. 4

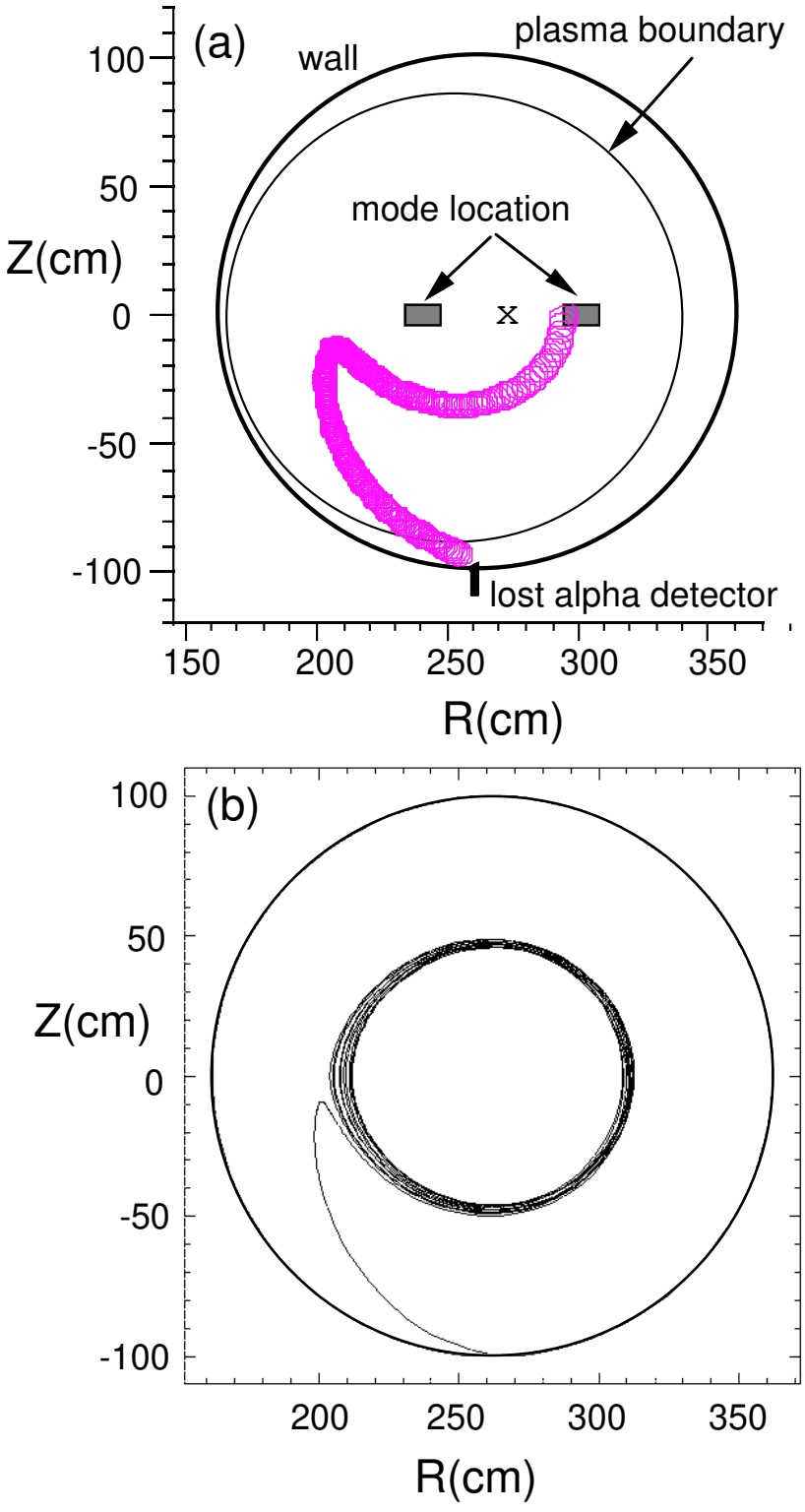
(a)
wall
plasma boundary
mode location
x
lost alpha detector
100
50
0
-50
-100
Z(cm)
150
200
250
300
350
R(cm)
(b)
100
50
0
-50
-100
Z(cm)
200
250
300
350
R(cm)

Fig. 5

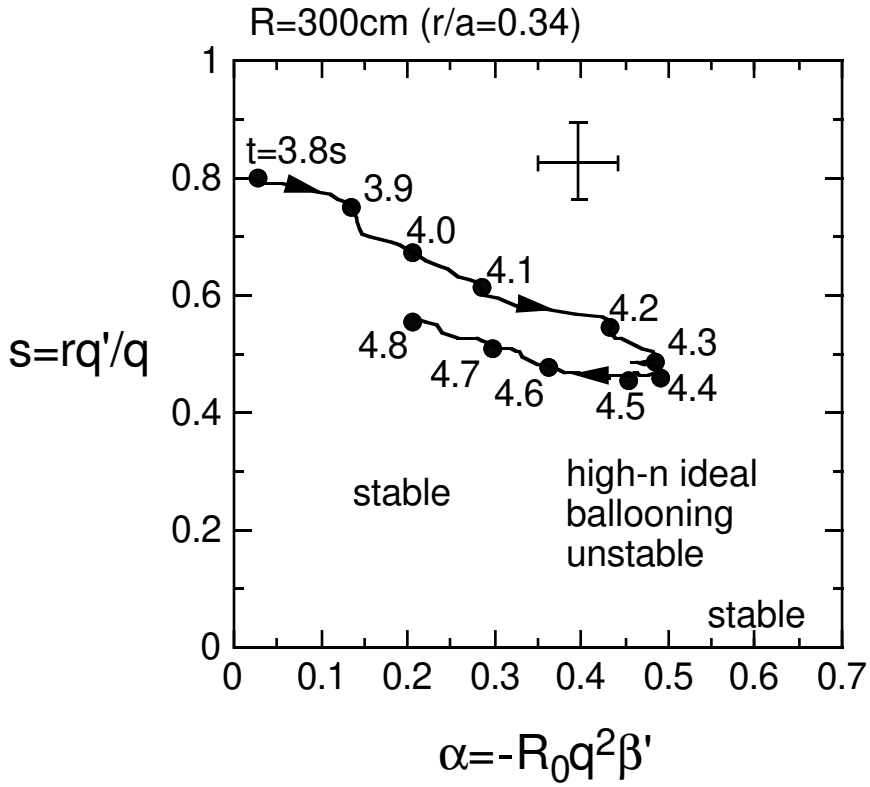
R=300cm (r/a=0.34)
s=rq'/q
α=-R0q2β'
t=3.8s
3.9
4.0
4.1
4.2
4.3
4.4
4.5
4.6
4.7
4.8
stable
high-n ideal
ballooning
unstable
stable
0
0.2
0.4
0.6
0.8
1
0
0.1
0.2
0.3
0.4
0.5
0.6
0.7

Fig. 6

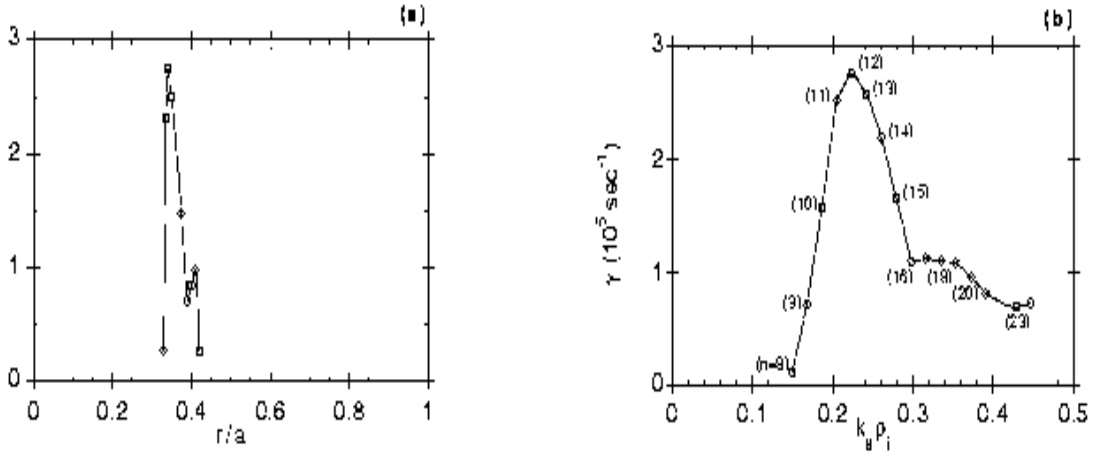
(a)
3
2
1
0
0
0.2
0.4
0.6
0.8
1
r/a
(b)
γ (10^5 sec^-1)
(n=9)
(9)
(10)
(11)
(12)
(13)
(14)
(15)
(16)
(18)
(20)
(23)
0
0.1
0.2
0.3
0.4
0.5
k_θ ρ_i

Fig. 7